Electronic Supplementary Material (ESI) for Energy & Environmental Science

Supplementary Information

A Universal Optical Approach to Enhanced Efficiency in Organic-based Photovoltaic Devices

Jason D. Myers[1], Weiran Cao[1], Vincent Cassidy[1], Sang-Hyun Eom[1], Renjia Zhou[1], Liqiang Yang[2], Wei You[2], and Jiangeng Xue[1]

[1] Department of Materials Science and Engineering, University of Florida, Gainesville, FL 32611, USA

[2] Department of Chemistry, University of North Carolina, Chapel Hill, NC 27599, USA

Detailed Device Structures:

For polymer:fullerene and hybrid devices, a poly(3,4-ethylenedioxythiophene):poly(styrenesulfonate) (PEDOT:PSS) (Clevios P) layer spin coated from an aqueous solution and subsequently annealed in air (140°C, 10 minutes) was the hole extraction layer. The active layers, and in some cases a ZnO nanoparticle layer, were spin coated in a nitrogen-filled glovebox with water and oxygen concentrations less than 0.1 ppm. Semi-transparent P3HT:PCBM devices used an electron-selective cathode of ITO/ZnO nanoparticles and a vacuum-deposited trilayer anode of MoO_3/Au/MoO_3 (3/10/40 nm). P3HT (Rieke Metals) and PCBM (Nano-C) were used as received. All P3HT:PCBM films were dissolved in chlorobenzene, at a ratio of 1:0.8 (by weight). P3HT:PCBM conventional devices without a ZnO layer were annealed for 30 minutes at 150°C in the glovebox after aluminum deposition. For conventional devices with a ZnO optical spacer, the P3HT:PCBM film was first annealed in the glovebox for 10 minutes at 115°C. The ZnO layer was then spin coated from an ethanol solution and annealed again at 115°C for another 10 minutes. Semi-transparent devices use a 40nm-thick electron-selective layer of ZnO spin coated on top of ITO, annealed at 85°C for 15 minutes in a nitrogen glovebox. After ZnO annealing, the active layer was spin coated and annealed at 150°C for 30 minutes in a glovebox.

High-efficiency devices were spin coated from solutions of 22 mg/mL, 1:1 (by weight) PBnDT-DTffBT:PCBM in dichlorobenzene on top of 40 nm-thick PEDOT:PSS. After spin coating, devices were solvent annealed for 12 hours in a closed petri dish inside of the glovebox; 1 nm LiF as an electron extraction layer and an aluminum cathode were deposited to complete the device. Finally, the hybrid inorganic/organic devices were spin coated from solutions of 9:1 (by weight) PCPDTBT (Luminescent Technologies):CdSe nanoparticles (~7 nm diameter) dissolved in a 9:1 chlorobenzene:pyridine solvent mixture on top of 40 nm-thick PEDOT:PSS. Devices were annealed inside a glovebox at 150°C for 30 minutes prior to aluminum cathode deposition.

Optical Field Dependence:

In Figure 1d of the main text, we show the effect of increased C_{60} layer thickness on device enhancement with and without a microlens array (MLA). In terms of absolute performance, the optimized thickness with a MLA remains at 12 nm boron subphthalocyanine chloride (subPc)/ 40 nm C_{60} despite the increased enhancement with thicker C_{60} layers, as shown in Figure S1.

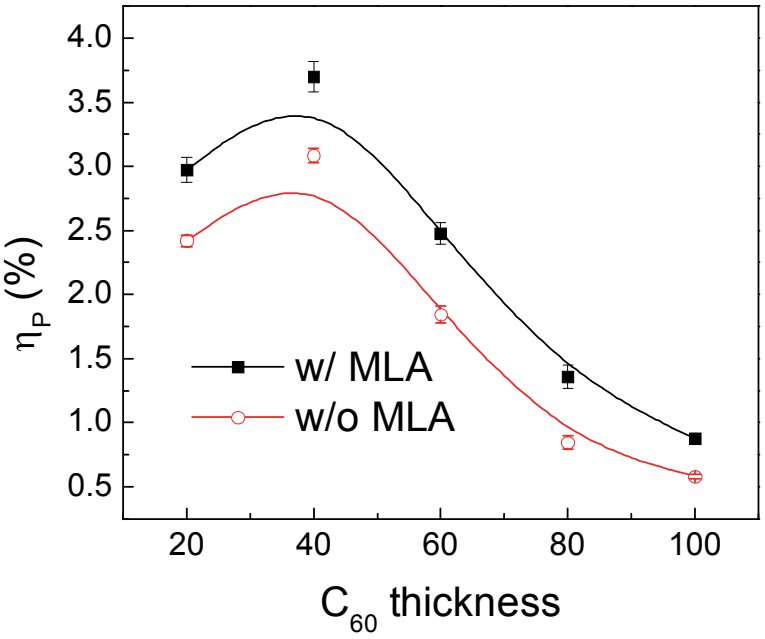

Figure S1 – Effect of increased C_{60} thickness on power conversion efficiency in a SubPc/C_{60} (12/*y* nm) with and without a microlens array.

Figure 1d of the main text also shows calculated enhancements in short-circuit current density using transfer matrix simulations; these are in general agreement with the experimental data. To obtain qualitatively significant data the calculated currents for several different incident angles must be averaged together, as a MLA does not equally refract all light to a single incident angle. Ray optics simulations were used to obtain a proper angular distribution. A custom simulation program was written that fires a large number of rays at a simulated device stack, both with and without a MLA. The propagation behavior of each ray is then tracked until it is absorbed within the active layer, reflected away from the stack, or transmitted through the back side of the stack, away from the device active area.

To determine the angular distribution, subPc:C_{60} (1:4 by weight) active layers of various thicknesses were simulated with 90° contact angle, 100 μm size microlens arrays. The device, microlens array, and illumination areas were treated as infinite by applying periodic boundary conditions. Mixed films were used in place of bilayer subPc/C_{60} films for computational simplicity. To correlate results, the total active layer thicknesses were compared (i.e. 20 nm subPc:C_{60} is comparable to 12 nm subPc/10 nm C_{60}). Whenever a ray is absorbed its path length through the active layer is recorded; the incident angle was back-calculated from the ratio of path length to film thickness. The results follow expectations from the Beer-Lambert law. For a very thin device, the proportion of light absorbed with an increased path length will be more significant. In a thicker device, a substantial percentage of light with no angular component will already be absorbed, making the relative contributions at with longer path lengths less significant. From these results, the relative contributions for rays binned into five different angle groups (centered around 9.6°, 22.4°, 35.2°, 48°, and 60.8°) are calculated and used to weight the short-circuit current values calculated using transfer matrix simulations. While this is an adequate method to approximate the relative enhancements with and without a MLA using the transfer matrix method, a more rigorous implementation is needed for full quantitative simulations.

To further visualize the effect of the optical field shift, Figure S2 shows the transfer matrix-calculated external quantum efficiency within the subPc layer of a bilayer subPc/C_{60} device (12/80 nm). Under normal incidence (0°, no MLA), the optical field within the peak subPc absorption region of 550-600 nm is weak due to the large C_{60} thickness. When the incident angle is changed to 30° (approximating a MLA), this region of the optical field is shifted into the subPc layer, drastically increasing the quantum efficiency. The enhancement in this case is not only due to the increased path length due to angular incidence; the optical field change is highly beneficial to device performance.

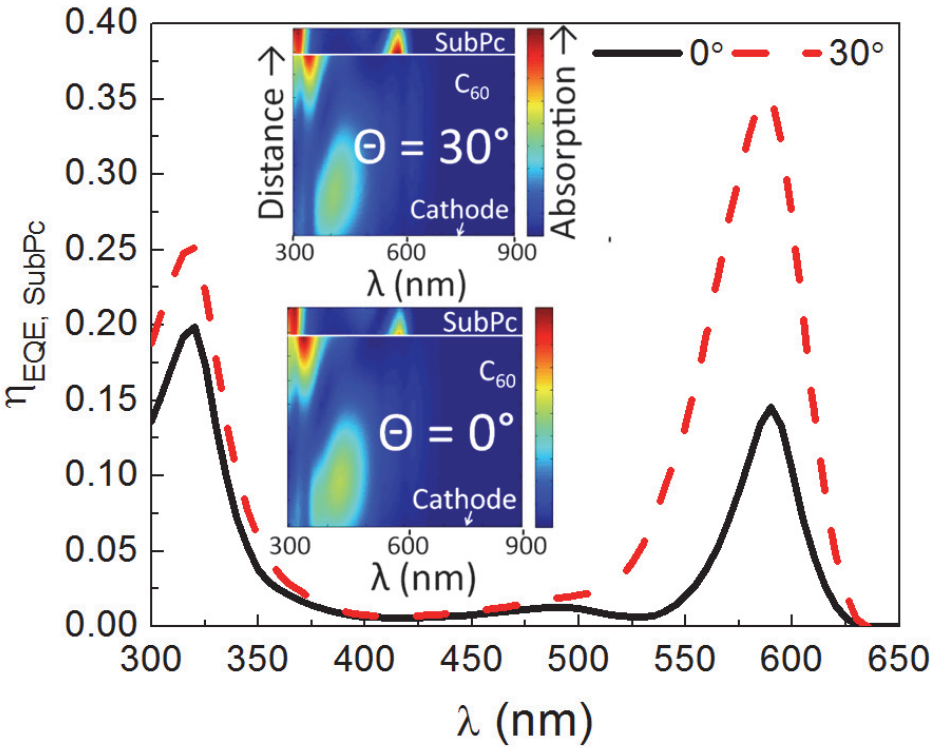

Figure S2 – External quantum efficiency calculated using transfer matrix simulations for a subPc/C_{60} (12/80 nm) at two different angles of incidence, to approximate a device with and without a microlens array. Inset: absorption intensity plot across the active layer at different illumination angles.

Geometric Enhancement Characteristics

Microlens arrays introduce several dependencies on the geometric relationship between the illumination, device, and lens array areas. These effects arise because the arrays diverge light in a periodic pattern over the illumination area. The even dispersion creates the favorable characteristic that enhancements increase with device area as loss mechanisms reduce. The effect of device area on J_{SC} enhancement for subPc/C_{60} (12/60 nm) bilayer devices is shown in Figure S3 for both large area illumination and device area illumination.

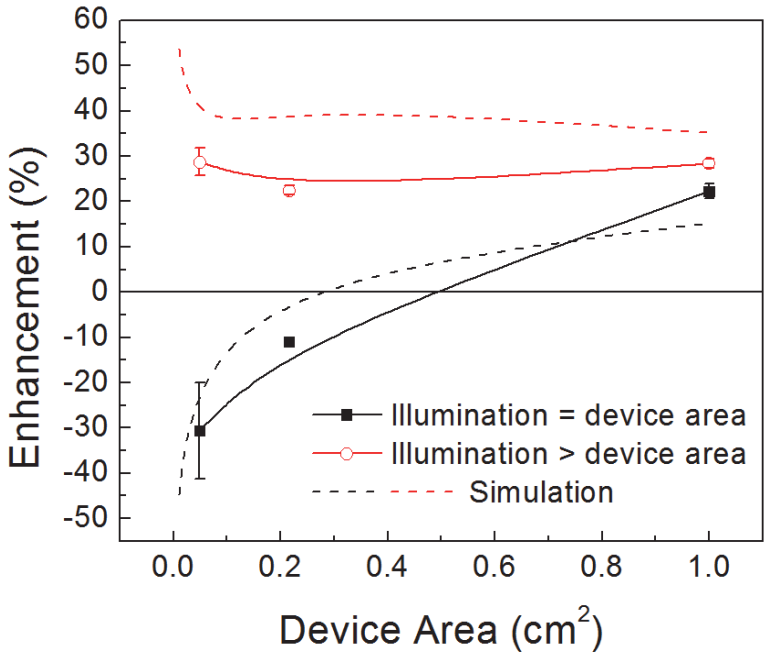

Figure S3 – Effect of device active area on relative enhancement with subPc/C_{60} (12 nm/60 nm) devices. Devices were either illuminated with a beam ~2" in diameter (large area illumination) or masked off so only the active area was exposed to light (device area illumination). Ray optics-simulated absorption enhancement in a 70 nm subPc:C_{60} (1:4) device is included.

Considering a device where the illumination area is equal to the device area, light near the edge of the device is refracted and diverted outside of the active area; with small, laboratory scale devices, the perimeter length is relatively long compared to the total device area and a large proportion of incident light will be lost. As the device active area becomes larger, the

proportion of light lost around the edges decreases accordingly. Extending the concept, an infinitely large device would not exhibit this effect. Lost light can be partially compensated for by making the illumination area larger than the device area, where light can be incoupled from outside of the device area. Ray optics simulations confirm this behavior.

This effect has important ramifications for production-scale devices. In the laboratory, device areas are typically kept small for ease of fabrication and characterization. Commercial devices, however, need to be as large as possible to maximize power generation and minimize module cost. Any optical enhancement technique should accordingly be compatible with large areas, as MLAs are.

Because of this effect, the devices results that we report in the main text are, unless otherwise noted, small area devices (~4 mm^2) with a large area reflector (2.25 cm^2). The rear reflector is isolated from the electrodes by a 100 nm-thick layer of Cytop fluoropolymer, a transparent insulator. In this arrangement, we are testing the electrical characteristics of a small area device that has the geometric characteristics of a large area device.